JOURNAL OF PROPULSION AND POWER
Vol. 17, No. 5, September–October 2001

# Electrospray as a Source of Nanoparticles for Efficient Colloid Thrusters

M. Gamero-Castaño* and V. Hruby†
*Busek Co., Inc., Natick, Massachusetts 01760-1023*

**The need for electric propulsion in the thrust range of tens of micro-Newtons has triggered the rebirth of colloid thruster technology. The ability to deliver thrust at these levels in a controllable fashion will enhance the use of small satellites (masses smaller than some 20 kg) and the execution of space missions in which very accurate positioning of spacecrafts is required. We present here a novel approach to the field of colloid thrusters. Like previous efforts it uses electrospray as the mean of producing charged colloids. However, it differs in the spraying regime employed. Electrosprays of highly conducting propellants in single cone-jet mode allow the generation of droplets of high specific charge at operating voltages lower than in the earlier era of colloid thruster research. In this article we use energy analysis techniques to characterize electrospray beams and to measure their thrust and specific impulse. We have studied three novel propellants: formamide, tributyl phosphate, and the ionic liquid 1-ethyl-3-methylimidazolium bis (trifluoromethylsulfonyl)imide. The thrust, specific impulse, and efficiency associated with a single spray of the most conducting formamide solution are typically 0.3 $\mu$N, 300 s, and 75% for an acceleration voltage of 1300 V. The electrospray phenomenology presented in this article is diverse. For example, by varying the electrospraying parameters we are able to study emission modes in which 1) solvated ions are field evaporated from the jet's surface, 2) both satellite and main droplets result from the jet's breakup, and 3) only main droplets are emitted.**

## Nomenclature

| | | |
|---|---|---|
| $D_d$ | = | droplet diameter |
| $E_n$ | = | normal component of electric field |
| $e$ | = | unity charge |
| $f(\varepsilon)$ | = | dimensionless function |
| $g$ | = | gravity's acceleration |
| $g(\varepsilon)$ | = | dimensionless function |
| $h$ | = | Planck's constant |
| $I$ | = | electric current |
| $I_{sp}$ | = | specific impulse |
| $J$ | = | field emitted ion flux |
| $K$ | = | liquid electrical conductivity |
| $k_B$ | = | Boltzman's constant |
| $L$ | = | length of flight |
| $m$ | = | molecular mass |
| $\dot{m}$ | = | mass flow rate |
| $\dot{m}_{FMT}$ | = | mass flow rate measured with flow meter |
| $\dot{m}_{TOF}$ | = | mass flow rate measured with time-of-flight (TOF) wave |
| $p_v$ | = | vapor pressure |
| $Q$ | = | liquid volumetric flow rate |
| $q/m$ | = | specific charge |
| $T$ | = | thrust |
| $t_F$ | = | time of flight |
| $V_A$ | = | acceleration voltage |
| $V_N$ | = | electrospray needle voltage |
| $\gamma$ | = | liquid surface tension |
| $\Delta G_S^0$ | = | ion solvation energy |
| $\varepsilon$ | = | liquid dielectric constant |
| $\varepsilon_0$ | = | vacuum permittivity |
| $\zeta$ | = | charge surface density |
| $\eta$ | = | efficiency |
| $\theta$ | = | absolute temperature |
| $\rho$ | = | liquid density |
| $\sigma$ | = | standard deviation |
| $\langle\rangle$ | = | mean value |

Received 14 July 2000; revision received 7 February 2001; accepted for publication 7 February 2001. 

*Research Scientist. Member AIAA.
†Chief Scientist. Member AIAA.

## I. Introduction

ELECTROSPRAY is a source of particles for efficient electrostatic propulsion. High electric fields applied to a liquid surface are known to deform it forming so-called Taylor cones.[1] If a proper liquid flow is fed to the cone simultaneously, a steady jet emanates from its apex, which eventually disrupts into charged droplets.[2,3] Although, using different combinations of experimental parameters, many electrospraying regimes are attainable, in this paper we will be entirely concerned with that known as cone-jet mode.[4,5] The diameter and specific charge of the droplets and the electric current emitted by a cone jet depend on the physical properties of the liquid (mainly its electrical conductivity, surface tension, and dielectric constant) as well as its flow rate. Two cone-jets are shown in Fig. 1. Liquid meniscus and spray of droplets are observed in both photographs. The jet issued from the cone's tip is not discernible because of the reduced dimension of its diameter. The hollow needle used to anchor the electrospray, feed the liquid, and set the required voltage difference with respect to a facing electrode is observed in Fig. 1b. In both photographs the electrosprayed liquid and the flow rate are the same. The background pressure is the only difference: the electrospray in Fig. 1a is held at atmospheric pressure, and the drag on the charged droplets exerted by the surrounding gas causes the large broadening of the spray. The electrospray in Fig. 1b is held under vacuum, and the expected reduction on spray's solid angle is apparent. Further angle reduction can be expected by charge neutralization, which would reduce electrostatic repulsion of the unipolar spray.

The research on the suitability of electrospray for space propulsion dates back to the early 1960s,[6,7] and continuous effort extended well into the next decade.[8] The colloid source most commonly used during this stage consisted of multijet, highly stressed electrosprays of glycerol. Because of the relatively poor conductivity of glycerol (see Ref. 9, where a 19.3% solution by weight of NaI in glycerol has an electrical conductivity of 0.021 S/m), very high onset voltages were required to obtain colloid beams with reasonable specific impulses (values of 10 kV were typical). Even though successful lab prototypes were eventually built,[10] interest in this technology decreased and eventually disappeared. Some factors that aborted this initial period of colloid thruster research can include: 1) the general downturn in space technology work in the post-Apollo era; 2) the improvement of classical Kaufmann ion engines, which delivered similar performance with less complexity; 3) the problematic high operating voltages required (>10 kV); and 4) the difficulty in

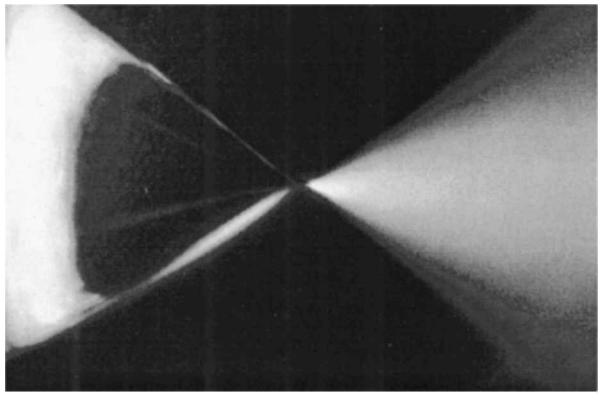

**Fig. 1a Electrospray of tributyl phosphate held at atmospheric pressure.**

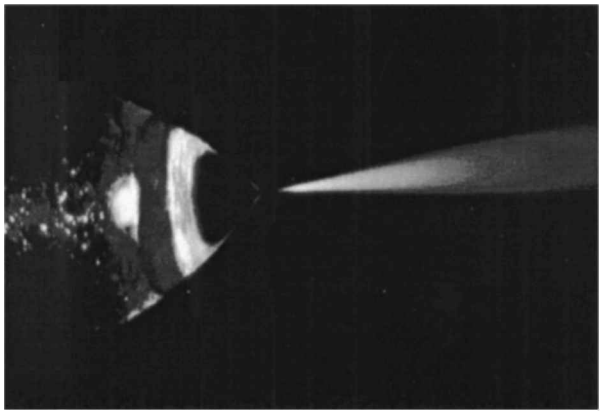

**Fig. 1b Electrospray of tributyl phosphate set under vacuum.**

scaling up to thrusts of many Micro-Newtons, which was the range of interest during those years. An extended review of the early effort in this field is contained in Ref. 11.

Several reasons have recently rekindled the interest in colloid thruster technology:

1) The low output thrust typical of a single electrospray is now seen as an advantage rather than a problem and is in fact essential in some missions as interest has increased for propulsion capability for smaller spacecraft.

2) The need for formation flying of multiple satellites whose relative positions must be precisely controlled calls for a propulsive scheme characterized by continuous microthrust levels, which also must offer the possibility of fine thrust variations. Only colloid and field emission thrusters are thought to yield this performance.

3) The knowledge gained during the last decade in the electrospraying of liquids allows now a reasonable understanding of the colloid generation. Use of more conducting solvents than glycerol enables the generation of sprays with the desired high specific impulse in the single cone-jet mode at onset voltages ($\sim$1.5 kV) much lower than previously. Furthermore, this new knowledge allows a confident design of the colloid source based on physical laws.

In this article we study the suitability of cone-jets as a source of charged particles for space propulsion. The main emphasis is on the characterization of the sprays emitted by a single source, the measurement of produced thrust and specific impulse, and the evaluation of several propellant candidates. The structure of the paper is as follows: after this introductory section we review some basic notions about electrosprays. This includes the scaling laws for the emitted current and droplet diameter and a brief discussion on the ion emission regime of cone-jets. The use of the time-of-flight technique to compute the propulsive characteristics of a colloid beam is described as well. Section III presents the experimental hardware and liquid propellants employed in this investigation. The discussion of the main experimental findings is given in Sec. IV. Finally, the article ends with some brief conclusions.

## II. Basic Characteristics of Cone Jets

The electric current and main diameter of the droplets ejected by cone jets have been reported in a variety of publications. The scaling laws for $I$ and $\langle D_d \rangle$ are[12–15]

$$I = f(\varepsilon)(QK\gamma/\varepsilon)^{\frac{1}{2}} \tag{1}$$

$$\langle D_d \rangle = g(\varepsilon)\left(Q\varepsilon\varepsilon_0/K\right)^{\frac{1}{3}} = g(\varepsilon)r^* \tag{2}$$

where $r^*$ is the characteristic length at which the fluid flow and electric times become comparable at the cone's apex.[12,16] Although the complexity of the electrospraying process handicaps the analytical calculation of $I$ and $\langle D_d \rangle$, asymptotic approximations have been obtained, which match the experimental data with reasonable success.[17,18] Furthermore, the authors of a recent numerical algorithm claim that the geometry of the cone-jet and its electric current can be solved accurately using their model.[19] Although there exists a general consensus about Eq. (1), Gañan-Calvo[17] and Hartman et al.[20] find a slightly different expression for the main droplet diameter $\langle D_d \rangle \sim Q^{1/2}/K^{1/3}$. However, this discrepancy with Eq. (2) is relatively irrelevant for the purpose of determining the mean diameter of actual electrospray droplets. In fact, the range of droplet diameters produced by the jet breakup, in conjunction with the limited resolution of most experimental techniques used to measure $\langle D_d \rangle$, makes it impossible to asses which expression for $\langle D_d \rangle$ is more appropriate. We will therefore regard hereafter Eqs. (1) and (2) as the most appropriate forms for the scaling laws.

From the point of view of electrospray operation, it is also of interest to know the range of flow rates in which a given solution forms stable cone-jets. It is known experimentally that the minimum $Q$ is such that[12]

$$\frac{\rho Q_{\min} K}{\gamma \varepsilon_0 \varepsilon} \sim 1 \tag{3}$$

while the maximum value is usually some 20–40 times larger than $Q_{\min}$.

Although Eq. (2) is important in many applications, knowledge of the diameter of electrospray droplets might seem to be relatively unimportant for colloid thrusters. Indeed, the main parameter in this case is the specific charge of the electrospray droplets rather than their diameters, and an average specific charge for the colloids can be computed from Eq. (1) alone as

$$\langle q/m \rangle = I/\rho Q \sim [f(\varepsilon)/\rho](K\gamma/Q\varepsilon)^{\frac{1}{2}} \tag{4}$$

Nevertheless, expression (2) is important also to colloidal propulsion. On the one hand, it is needed to have a good understanding of the electrospraying process. On the other hand, the knowledge of the jet curvature is essential to characterize the emission of ions from Taylor cones. In fact, under appropriate conditions, cone-jets not only produce charged droplets, but they also field evaporate ions.[21] This happens when the normal electric field at the jet surface reaches a value of the order of 1 V/nm. The maximum value of the normal electric field $E_n^*$ is located at the tip of the liquid meniscus in the region where the jet begins to develop. Using the expression for the jet's radius of curvature, the scaling law for $E_n^*$ is written as[21]

$$E_n^* \sim \left(\frac{\gamma}{\varepsilon_0 r^*}\right)^{\frac{1}{2}}, \qquad E_n^* = \varphi \frac{\gamma^{\frac{1}{2}} K^{\frac{1}{6}}}{\varepsilon^{\frac{1}{6}} \varepsilon_0^{\frac{2}{3}} Q^{\frac{1}{6}}} = \varphi E_K \tag{5}$$

where the constant $\varphi$ of order unity is still unknown although it could be obtained through experiments or analytical modeling. It is observed that $E_n^*$ increases for decreasing flow rate and increasing

conductivity. In particular, $E_n^*$ is proportional to $K^{1/3}$ for cone-jets of a given liquid matrix when they are set close to the minimum flow rate. For the case of ions evaporating from the surface of a dielectric liquid, the field emitted current flux is well approximated by[22]

$$J = (k_B\theta/h)\zeta \exp\left\{\left[\Delta G_S^0 - \left(e^3 E_n \big/ 4\pi\varepsilon_0\right)^{\frac{1}{2}}\right] \big/ k_B\theta\right\} \tag{6}$$

Notice that the current flux depends exponentially on the electric field normal to the surface. Hence, it is expected that once the flow rate and electrical conductivity in the cone-jet are such that ions are field evaporated, small changes in the flow rate, i.e., small changes in $E_n^*$, will bring about large variations in the ion yield. This phenomenology will be described in Sec. IV.

The preceding paragraphs are aimed to guide those readers unfamiliar with the field of electrospray and might have obscured the main objective of this paper, i.e., the study of the suitability of cone jets as colloid thrusters. Terms such as thrust, mass flow rate, specific impulse, and efficiency are most important in the propulsive arena. The scaling law (1) can be used to obtain approximate relations for the thrust and specific impulse yielded by electrosprays:

$$T \sim [2V_A \rho f(\varepsilon)]^{\frac{1}{2}} (K\gamma Q^3/\varepsilon)^{\frac{1}{4}} \tag{7}$$

$$I_{\rm sp} \sim (1/g)[2V_A f(\varepsilon)/\rho]^{\frac{1}{2}} (K\gamma/Q\varepsilon)^{\frac{1}{4}} \tag{8}$$

For a propellant of fixed conductivity, the increase of flow rate translates into larger thrust output. Unfortunately this is accompanied by a penalization of specific impulse. If the preceding equations are complemented with the information about the range of operational flow rates, i.e., expression (3), the dependence of thrust and specific impulse on solution conductivity is $T \sim K^{-1/2}$ and $I_{\rm sp} \sim K^{1/2}$. When emphasis is placed on the specific impulse associated with the electrospray beam, the importance of working with propellants of high electrical conductivity is apparent.

If more accurate values of $T$ and $I_{\rm sp}$ are required, special tools must be developed. Traditionally, the so-called time-of-flight technique (TOF) has been of great help for measuring $T$, $\dot{m}$, $I_{\rm sp}$ and $\eta$ of charged, colloid beams accelerated by an electric field.[23] A TOF measurement is a time-dependent spectrum of a current signal associated with the electrospray beam $I(t)$ following its instantaneous interruption. The analysis of $I(t)$ yields the specific charge distribution function of the electrospray particles, provided that their acceleration voltage is known. Furthermore, by proper integration of $I(t)$ the thrust, mass flow rate, specific impulse, and efficiency can be computed:

$$T = \int_0^\infty \frac{2V_A(t)}{L} t I' \, dt \tag{9}$$

$$\dot{m} = \int_0^\infty \frac{2V_A(t)}{L^2} t^2 I' \, dt \tag{10}$$

$$I_{\rm sp} = \frac{T}{\dot{m} g} \tag{11}$$

$$\eta = \frac{T^2}{2\dot{m} V_N I} \tag{12}$$

It is desirable to use a thrust balance to measure $T$. However, no balance capable of measuring the thrust values characteristic of a single cone jet (typically of the order of 0.5 $\mu$N) is available. Furthermore, even if a thrust stand could be used, it seems that the simultaneous measurement of $T$ and $\dot{m}$ required to calculate the specific impulse would be extremely difficult.

## III. Experimental Hardware

We have studied electrosprays under vacuum conditions using the setup shown in Fig. 2. The electrospray needle is installed inside a 5 cm cross, which is mounted on a 46 cm diam tank. A background pressure of $10^{-5}$ torr, low enough to carry out the experiments that will be described in Sec. IV, is achieved by means of a 30 cm diffusion pump backed by a 150 scfm mechanical pump. The solution to be electrosprayed is held in a plastic container. The pressure difference between this container and the electrospray chamber is controlled and measured by means of a vacuum pump, a compressed air line, and a barometer. The liquid is fed to the spraying needle through a line of fused silica of 100-$\mu$m i.d. This line is used as a bubble flow meter for measuring the flow rate of every experimental run: a bubble of air is inserted in this capillary, and the flow rate is measured by monitoring its displacement in a given time. The major source of error in the flow rate measurement is given by the tolerance for the i.d. of the capillary, $100 \pm 6$ $\mu$m (Polymicro Technologies, 18019 N. 25th Ave., Phoenix, AZ 85023). Thus, the uncertainty of this flow meter's measurements is approximately 12%. The flow meter is connected to a second line, which, when properly sharpened, is used as an electrospraying needle. This second tube is also made of fused silica. We have used needles with different i.d.s, depending on the hydraulic resistance required to feed the very disparate flow rates associated with different liquid solutions (e.g., 22-$\mu$m i.d. lines were used for all formamide solutions, whereas tubes with 50-$\mu$m i.d. were employed for most tributyl phosphate samples). The needle tip must be sharpened into a cone and made electrically conducting (we deposit a layer of tin oxide on the needle chamfer to make it conductive). An 80× optical microscope equipped with a color video camera is used to observe the needle tip on a nearby TV monitor.

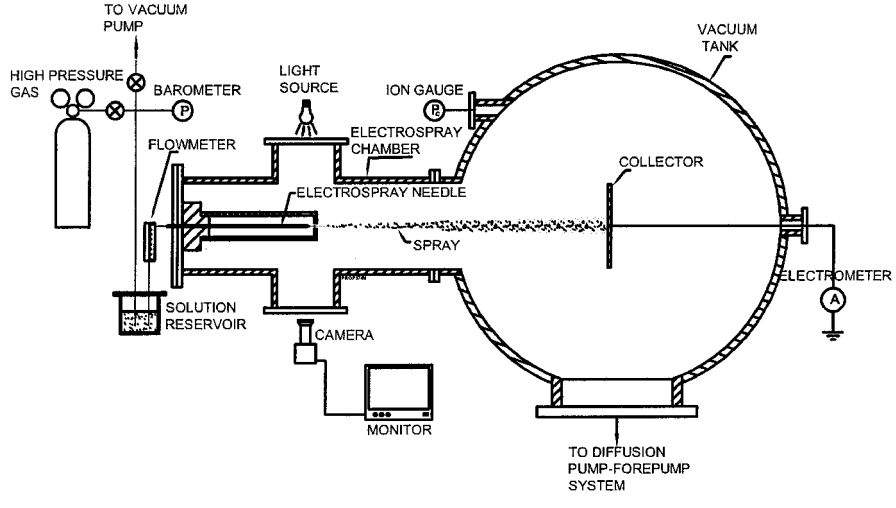


**Fig. 2 Schematic of the hardware used in this research to study electrosprays.**

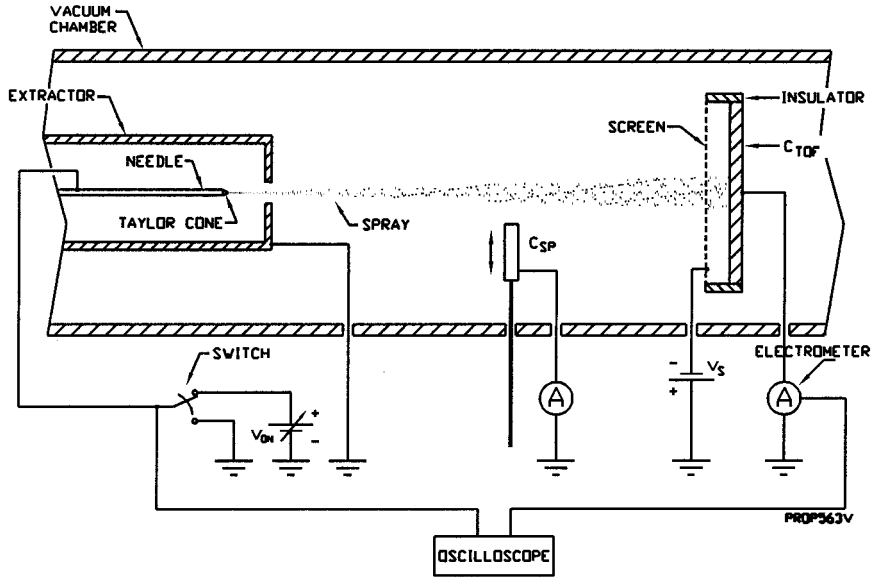


**Fig. 3 Sketch of the electrode geometry and electric connections employed to record time of flight spectra of colloid beams.**

To form a cone-jet, an appropriate voltage difference between the electrospray needle and a nearby electrode, extractor hereafter, must be set. Furthermore, because the electrospray beam has to be studied far from its emission point, the extractor must allow the passage of the entire beam. This electrode arrangement and the TOF apparatus are shown in Fig. 3. The charged beam exiting the extractor-needle region enters a drift section of null electric field and eventually reaches a collector $C_{\mathrm{TOF}}$, connected to a fast electrometer. A screen of high porosity (0.3-mm square openings, 5 mm apart from the collector) is biased negatively to eliminate spurious currents associated with secondary electrons emitted by highly energetic particles impinging in the collector. A high-speed, high-voltage switch is used to periodically short the needle voltage to ground. The falling time of the needle voltage is 0.4 $\mu$s, much smaller than the time of flight of the droplets we measure in this paper. During the interval in which the needle is shorted, the electrospraying process is interrupted, and a beam wake moves toward the collector. The TOF of this wake can be easily measured by means of an oscilloscope connected to the electrometer output and triggered by the voltage signal of the electrospray needle. The electrometer's settling time to 0.01% is 2 $\mu$s, fast enough for measuring these electrospray beams. The specific charge of the beam particles is computed from the values of their times of flight, drift length, and acceleration voltage:

$$q/m = (1/2V_A)(L/t_F)^2 \tag{13}$$

Because the electrospraying process generates particles within a range of specific charges and acceleration voltages, the TOF spectra recorded by the oscilloscope will resemble combinations of error-function-like curves with different widths, rather than step functions.

Unfortunately, the acceleration voltage of the beam particles is not simply the voltage of the electrospray needle $V_N$. In fact, droplets with different acceleration voltages are generated at the jet breakup. Voltage losses as large as 500 V have been measured previously for tributyl phospate solutions of low conductivity ($K = 10^{-5}$ S/m). (Ref. 24). The difference $\Delta = V_N - V_A$ is associated with both electric conduction losses in the cone jet and changes in the sum of kinetic and potential energies of the fluid occurring during the acceleration of the jet and its breakup. The acceleration voltage of the electrospray particles can be measured using the so-called stopping potential technique.[9,24] We have used the experimental setup shown in Fig. 4 to carry out stopping potential measurements. A cone-jet is set at the tip of the electrospray needle by applying a voltage difference $V_{\mathrm{ON}}$ between needle and extractor. The electrospray beam is directed toward a collector $C_{\mathrm{SP}}$, at which its electric current can be measured. This collector is virtually grounded through the electrometer. The acceleration voltage of the emitted droplets can be varied by means of a power supply connected between ground and the extractor. Hence, by reducing the voltage of the extractor while keeping constant $V_{\mathrm{ON}} = V_N - V_E$ we will have a stable cone jet that eventually emits droplets at ground voltage. At this moment no more current is measured by the electrometer, and the voltage of the needle is equal to $\Delta$. Because $\Delta$ is fairly independent of $V_{\mathrm{ON}}$ in the onset voltage range at which stable cone-jets are formed, the acceleration voltage for any value of the voltage needle is simply $V_N - \Delta$. An electrode labeled "lens" in Fig. 4 was used to deal with secondary ionization prompted by the electrosprays of most conducting solutions, which are partially formed by high energetic ions.[21] Finally, in order to measure simultaneously the time of flight and stopping potential spectra of a given spray the collector $C_{\mathrm{SP}}$ could be displaced to either intercept or allow the passage of the electrospray beam (see Fig. 3).

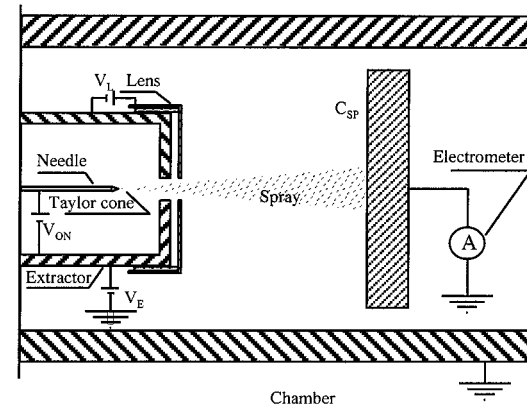


**Fig. 4 Sketch of the set electrodes used to measure the stopping potential of electrospray droplets.**

We have used the experimental tools just described to study the suitability of several solutions as propellants for colloid thrusters. The low-pressure environment inherent with electrostatic propulsion imposes a constraint on the vapor pressure of these liquids. Liquids such as glycerol and octoil were preferentially studied in the 1960s and 1970s for this application. In this work we have studied other compounds that were not targeted in the earlier era of colloid thruster research: formamide, tributyl phosphate (TBP), the ionic liquid 1-ethyl-3-methylimidazolium bis (trifluoromethylsulfonyl)imide (Emi-Im),[25] and mixtures of Emi-Im with TBP. When compared with glycerol solutions, mixtures of formamide and salts

**Table 1 Solutions studied in this work**

| Solution | Salt concentration, %w | Electric conductivity, S/m | Density, kg/m$^3$ |
|---|---|---|---|
| F1 | Form[a]-(1.73%w) NaI[b] | 0.22 (19°C), 0.30 (21°C) | 1153 |
| F2 | Form-(6.33%w) NaI | 0.63 (19°C), 0.81 (21°C) | 1187 |
| F3 | Form-(11.8%w) NaI | 0.93 (19°C) | 1234 |
| F4 | Form-(16.8%w) NaI | 1.23 (19°C), 1.50 (23°C) | 1289 |
| TBP1 | TBP[c]-(1.52%w) TBATPB[d] | 0.0085 (22°C) | 976 |
| TBP2 | TBP-(7.30%w) Emi-Im[e] | 0.096 (22°C) | 1012 |
| TBP3 | TBP-(14.3%w) Emi-Im | 0.14 (22°C) | 1038 |
| TBP4 | TBP-(39.0%w) Emi-Im | 0.33 (22°C) | 1150 |
| Emi-Im | Pure Emi-Im | 1.01 (24°C) | 1460 |

[a]Formamide. [b]Sodium Iodide. [c]Tributyl phosphate.
[d]Tetrabutylammonium tetraphenyl borate.
[e]1-ethyl-3-methylimidazolium bis (trifluoromethylsulfonyl)imide.

have the advantage of reaching much higher electrical conductivities, and thus their cone-jets produce charged particles of improved specific charge and specific impulse. Ionic liquids are virtually involatile, and some of them have the large conductivities appropriate for colloid thrusters. Many others reach reasonable conductivities when mixed with less viscous, involatile organic solvents. The diversity of pure ionic liquids and their possible combinations offer a virgin ground in the research of colloid thrusters and in other applications where the production of nanoparticles is desired. We must point out that the possible suitability of ionic liquids as colloid propellants, both as part of mixtures with other organic liquids or at enhancing temperatures, is an original idea of Professor Fernández de la Mora (Mechanical Engineering Department, Yale University). We have studied in this paper mixtures of formamide and sodium iodide of different concentrations, TBP and Emi-Im. The nature of these solutions, their densities, and electrical conductivities are given in Table 1. We did not observe noticeable changes in the nature of the solutions throughout the time the experiments were carried out. However, the electrical conductivity of these solutions depends strongly on their temperature, especially for the most viscous liquid (Emi-Im).

It could be argued that the evaporation of mass from the flying droplets might cause important errors in the determination of the specific charge and stopping potential of electrospray droplets. However, this is not the case. For a drop in free-molecule conditions and constant temperature, the rate of change in diameter as a result of mass evaporation is given by[26]

$$\frac{\mathrm{d}D_d}{\mathrm{d}t} = -\frac{2m^{\frac{1}{2}} p_v(\theta)}{\rho(2\pi k_B \theta)^{\frac{1}{2}}}$$

For formamide we have $p_v(293) = 1.9$ Pa, $m = 45.04$ amu, and $\rho = 1133$ kg/m$^3$ (Ref. 27). Thus, the rate of diameter variation is $-5.75$ $\mu$m/s. In our experimental setup the TOFs of formamide droplets are of the order 0.1 ms, and therefore the typical variation in diameter caused by mass losses is of some of 0.6 nm. On the other hand the initial diameter of the droplets is of the order of 30 nm or larger. Clearly, evaporative mass losses do not induce a major error in the determination of the specific charge of formamide droplets. The measurement of the stopping potential is even less affected because the distance between $C_{SP}$, and electrospraying needle is $\sim$10 times shorter than between $C_{TOF}$ and needle. For TBP droplets we have $p_v(293) = 0.58$ Pa, $m = 266.3$ amu, $\rho = 976$ kg/m$^3$, and accordingly $\mathrm{d}D_d/\mathrm{d}t = -4.96$ $\mu$m/s. The TOF is typically 1 ms, and therefore the variation in diameter is of some 5 nm. This variation is negligible because the initial diameters of the TBP droplets measured in this article are typicallly 0.1 $\mu$m or larger. For the case of ionic liquids, their vapor pressures are so small that $p_v$ is virtually an unmeasurable quantity. Furthermore, it is worth pointing out that the actual vapor pressures of formamide and TBP for the evaporating charged droplets is most likely lower than our estimates of 1.9 and 0.58 Pa. This is caused by two reasons: first, as liquid evaporates the droplet cools down because the gas mean free path in the vacuum chamber is too large to significantly thermalize the droplet by collisions. The cooling of the droplet lowers the vapor pressure, which is an exponential function of $T$. Second, the presence of surface charge lowers the vapor pressure of the liquid.[24] Theoretically, the vapor pressure of droplets charged at the Rayleigh limit is null. Finally, the irrelevance of mass evaporation from droplets in flight is proved by the fair agreement between the electrosprayed mass flow rates measured by both bubble flowmeter and TOF waves [Eq. (10)]. We will treat in more detail this point in Sec. IV.

## IV. Results

### A. Colloid Beam Phenomenology

This section begins with the description of TBP1 and F4 electrosprays. The energy analysis techniques presented in Sec. III will resolve the different types of charged particles within the colloid beams: main and satellite droplets for TBP1 and main droplets and solvated ions for the case of F4. Figures 5 and 6 show TOF and stopping potential spectra for solution TBP1. Curves associated with different TBP flow rates are plotted in each graph. TOF spectra are given in the form of current measured at $C_{TOF}$ as a function of time. For $t < 0$ the cone jet is operated steadily, and its current is recorded by the electrometer. At $t = 0$ the needle voltage is shorted to ground, and the spray is interrupted. Because the droplets travel toward $C_{TOF}$ with a finite speed $v$, it takes a time $L/v$ for the electrometer to measure null electric current. The width of the resulting error-function-like spectrum is a measure of the specific charge polydispersity of the particles in the spray. Stopping potential curves are plotted as current measured at $C_{SP}$ as a function of needle voltage (the voltage value of $C_{SP}$ is the reference voltage or ground). When $V_N$ is much lower than 0, the droplets will not reach $C_{SP}$ and null electric current is measured. On the other hand, for large $V_N$ every droplet has enough energy to reach $C_{SP}$, and the total electrospray

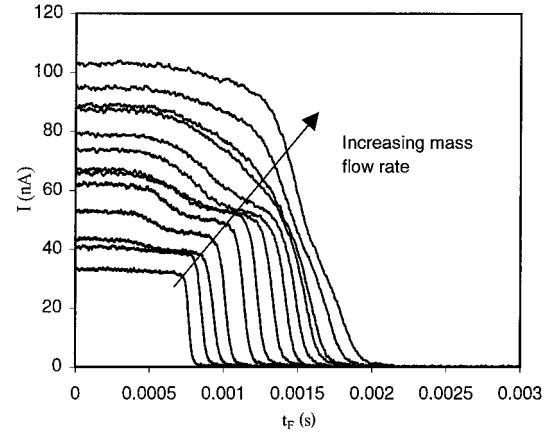


**Fig. 5 Time of flight curves for solution TBP1. Each curve is associated with a different liquid flow rate.**

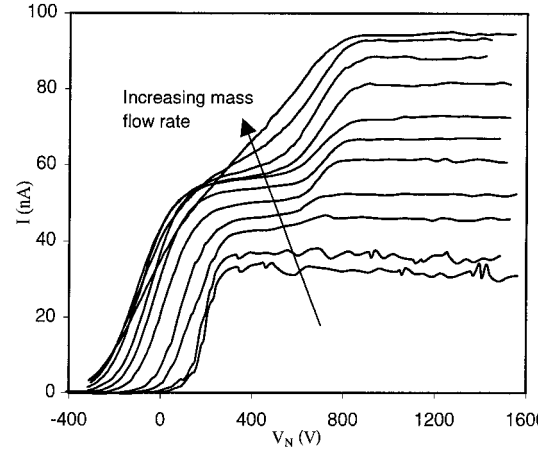


**Fig. 6 Stopping potential curves for solution TBP1. The evolution of droplet patterns is equivalent to that in Fig. 5.**

current is measured. At intermediate values of $V_N$, $V_A$ equals zero, and current begins to be sensed by the electrometer. As $\dot{m}$ increases, or equivalently as the spray current increases, a pattern of different types of droplets evolves similarly in both graphs: at low $\dot{m}$ there is only one step in the TOF and stopping potential curves, and hence only one type of droplets (main drops formed at the jet breakup) exists in the spray. At $I \sim 40$ nA a second step appears, which is associated with satellite drops formed at the jet breakup. Based on stopping potential analysis alone, this second step was previously[24] interpreted as being caused by the smallest drops resulting from Coulomb disintegration of main droplets in flight: it seemed unlikely that both satellite and main droplets, formed at the same jet breakup point, could have so different voltage losses. The TOF data are more definitive, for if the new step were caused by the products of Coulomb explosions a third step (the bigger product of the Coulomb explosion of the main drops, the former having a specific charge lower than the latter) should appear in the TOF curves. But this is not so, and we must conclude that the new step is associated with satellite droplets. The clear distinction observed in the TOF and stopping potential spectra between the prints of satellite and main droplets can be used advantageously to measure parameters such as the voltage drop along the cone jet and the velocity and diameter of the jet at the breakup location. This analysis will be presented elsewhere. A second transition in the spray spectra is observed at $I \sim 87$ nA. This coincides with the onset of a new jet oscillation mode known in the specialized literature as kink instability.[20] Notice the narrowness of the descending steps in the TOF curves, especially in the intervals associated with main droplets. Thus, for the case of $I = 33$ nA the variance of this error-function-like TOF spectrum is $\sigma^2 = 1.23 \times 10^{-9}$ s$^2$ [we have defined its distribution density function as $1/I(-\infty)(\mathrm{d}I/\mathrm{d}t)$] its mean value $\langle t_F \rangle = 7.55 \times 10^{-4}$ s, and the standard deviation $\sigma = 3.51 \times 10^{-5}$ s. If we assume that all of the droplets have the same acceleration voltage, then the mean specific charge, variance, and standard deviation are $\langle m/q \rangle = 0.0240$ kg/C, $\sigma^2 = 5.75 \times 10^{-6}$ kg$^2$/C$^2$, and $\sigma = 0.0024$ kg/C. In fact, the actual value of the specific charge deviation is probably smaller because of the artifice of using a constant acceleration voltage for all of the droplets (the width of the distribution of voltage losses is of the same order as the width of the TOF curve). Thus, it is a good approximation to regard all of the main droplets emitted by these cone jets as having the same volumetric charge, in spite of their relatively wide diameter distribution functions (the full width at half maximum is typically 30% of the mean[28]). This striking observation confirms with increased resolution the earlier data of Ref. 28. It indicates that most of the electric current in the vicinity of the jet breakup moves in the form of convected surface charge, rather than being conduction current (charge frozen at the surface scenario). Furthermore, the droplet formation time at the jet breakup must be much shorter than the time for an efficient redistribution of surface charge in the jet breakup region.[28] This is in clear contradiction with the hypothesis of jet breakup at constant voltage considered in recent research papers in which the droplet formation in cone jets is numerically studied.[20,29] If the breakup were equipotential, the specific charge of the main droplets would vary noticeably within a given electrospray [$q/m(D_d)$ should be roughly proportional to $1/D_d^2$], which is not observed.

The particle emission patterns just described change when more conducting solutions are electrosprayed. In fact, for high enough values of the ratio $K/Q$ the electric field at the jet exceeds the level required to field evaporate ions from the cone-jet surface at measurable rates. Figures 7 and 8 contain TOFs and stopping potential spectra for F4. The presence in the electrospray of two types of particles is observed in Fig. 7. Although the TOFs associated with the slower entities (main droplets) decrease as the spray current diminishes, the TOF of the second class remains constant regardless of the spray current. The specific charge of the latter is 84,700 C/kg (1137 Daltons). It is hard to imagine how multiply charged droplets could be produced having such large specific charge, which furthermore is constant in a wide range of flow rates. These particles must be highly solvated ions. The specific charge value $q/m = 84{,}700$ C/kg could be an underestimate because of the finite settling time of the

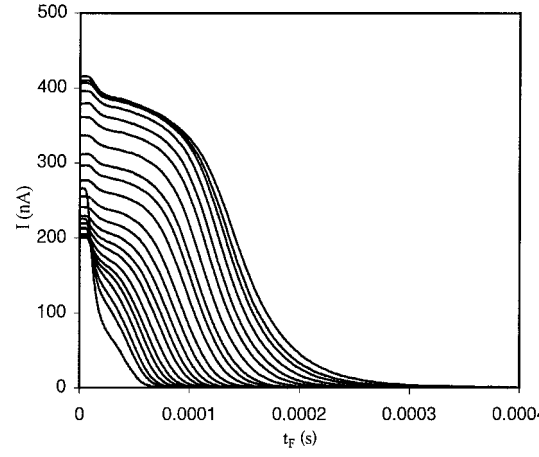


**Fig. 7 Time of flight spectra for solution F4. Solvated ions and main droplets appear at different times.**

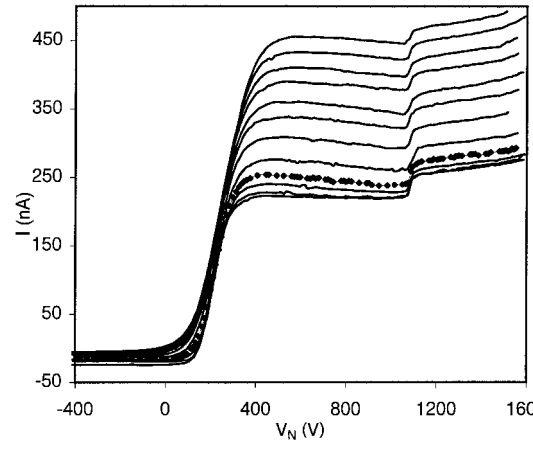


**Fig. 8 Stopping potential curves for F4. Ions and main droplets are collected in the same step (centered around $V_N = 200$ V) of the curves.**

electrometer and the indeterminacy in the measurement of the ion stopping potential. If we use the initial TOF ($\sim$10.4 $\mu$s) at which the ion wave begins to be sensed and the larger stopping voltage ($\sim$400 V) of the curves in Fig. 8, we obtain a maximum specific charge for the solvated ions of 176,000 C/kg. The TOF diameter of these solvated ions, $D = (6m/\pi\rho)^{1/3}$, $m = 1.89 \times 10^{-24}$ kg, $\rho = 1153$ kg/m$^3$, is 1.41 nm (1.10 nm for 176,000 C/kg), not far from the Born diameter

$$D_{\mathrm{Born}} = \left[ \frac{e^2(1 - \varepsilon^{-1})}{8\pi^2 \varepsilon_0 \gamma} \right]^{\frac{1}{3}} \tag{14}$$

which in this case is 0.86 nm. Born's expression (14) is a mere approximation based on energy considerations alone.

The evolution of the ion current as a function of the mass flow and the electric field $E_K$ defined in Eq. (5) is plotted in Figs. 9a and 9b. The total current emitted by the cone jets of F4 is also plotted in Fig. 9a in order to show the relative importance of the droplet and ion fractions. Notice that the ion yield is approximately constant at large flow rates and increases rapidly as the mass flow decreases below $3.7 \times 10^{-11}$ kg/s, $E_K = 1.09$ V/nm. This observation is consistent with a two-stage emission scenario: at large flow rates ions are emitted from either a fraction of the droplets having the larger electric fields or from the thin liquid filaments connecting the droplets at the very last stages of the jet breakup.[21] In both cases the total ion current must remain a small fraction of the total current: if the emission occurs from some droplets, the evaporated charge is a fraction of the droplet charge; if the emission occurs from liquid filaments, the very short breakup times preclude any

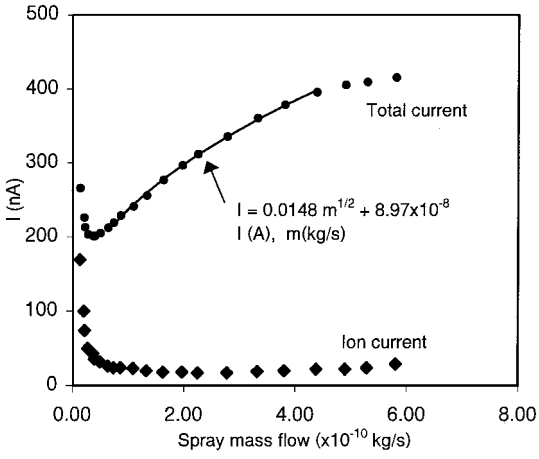


**Fig. 9a Ion yield as a function of mass flow rate for solution F4. At large flow rates there exists a residual ion current, which increases steeply below $\dot{m} = 3.7 \times 10^{-11}$ kg/s.**

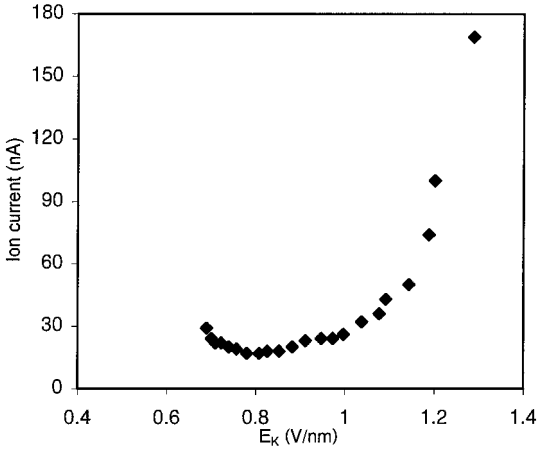


**Fig. 9b Ion yield as a function of electric field at the cone-jet apex for solution F4. The electric field $E_K$ is defined in Eq. (5). A critical value of $E_K$ (1.09 V/nm) triggers the onset of ion evaporation from the cone's apex.**

reorganization of the surface charge distribution. At low flow rates the electric field at the cone tip, where the jet begins to develop, is large enough to promote ion emission. The ion yield from this point is not limited in principle because the total electric current in the jet has not been fixed yet, and it is connected to the power supply by a resistive path (see Ref. 21 for a quantitative study of this ion-droplet emission regime). The stopping potential curves shown in Fig. 8 are used to assign an accurate acceleration voltage to the sprays studied by TOF. All of the particles presented in the sprays are collected in the low-voltage step of the curves and hence have a mean voltage loss of roughly 200 V. Notice the appearance of an additional step at 1100 V. It is caused by secondary ionization effects within the electrospray chamber. The reader interested in a more detailed description of these stopping potential curves is referred to Ref. 21.

### B. Measurement of Thrust and Specific Impulse

We use now Eqs. (9) and (10) to compute the thrusts and mass flow rates of these electrosprays. Figures 10–13 show the accumulated $T$ and $\dot{m}$ (i.e., the value of the integrals in Eqs. (9) and (10) between $t = 0$ and $t_F$) for several experimental runs obtained with solutions TBP1 and F4. To allow a proper comparison, the inverse of specific charge is taken as abscissa coordinate, rather than the TOF; this involves a straightforward change of variables from $t_F$ to $m/q$ Eq. (13). Evidently, the thrust and mass flow rate associated with each spray are the constant values reached at large $m/q$. The acceleration voltage of a given type of particle (main droplets, satellite

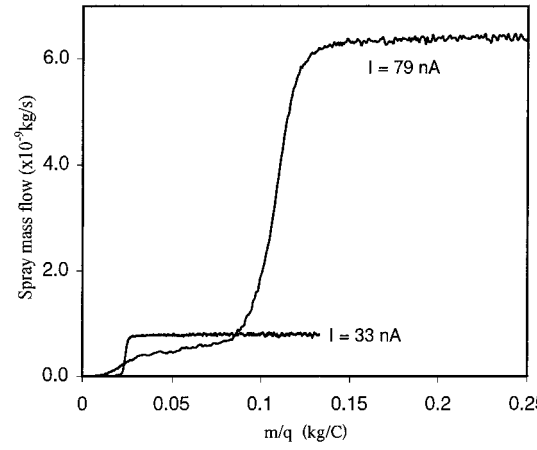


**Fig. 10 Beam mass flow of two TBP1 sprays. They have been computed by integrating their TOF spectra [Eq. (10)].**

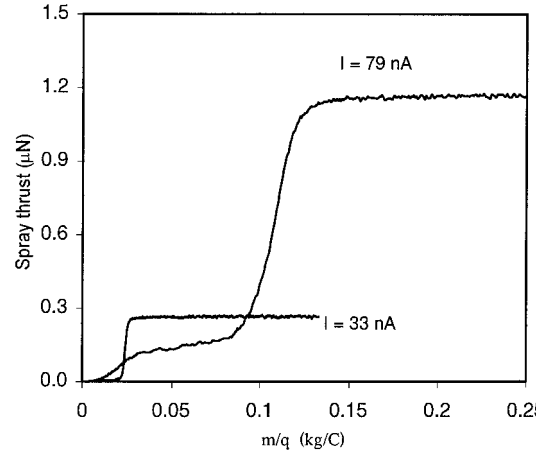


**Fig. 11 Thrust values rendered by time of flight analysis for the sprays in Fig. 10.**

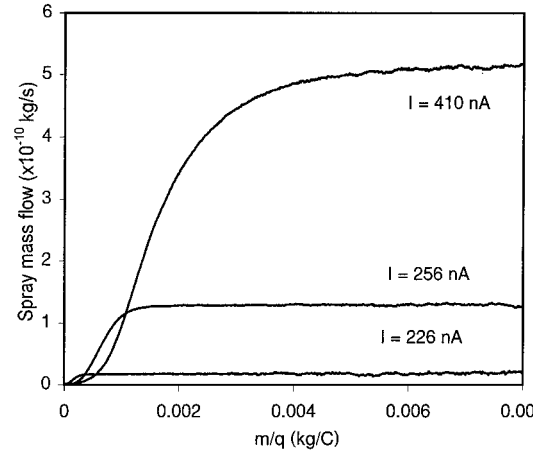


**Fig. 12 Beam mass flow of three F4 sprays, computed by means of Eq. (10).**

droplets, or ions) present in a given spray is taken to be the voltage of the electrospray needle minus the mean voltage loss yielded by the stopping potential curve for that particular particle and spray. Thus, although different types of particles in the same spray can have different acceleration voltages all of the particles of the same kind in a given spray are assigned a unique acceleration voltage, and particles of the same type but in different sprays (different flow rates) can have different acceleration voltages. Figures 14 and 15

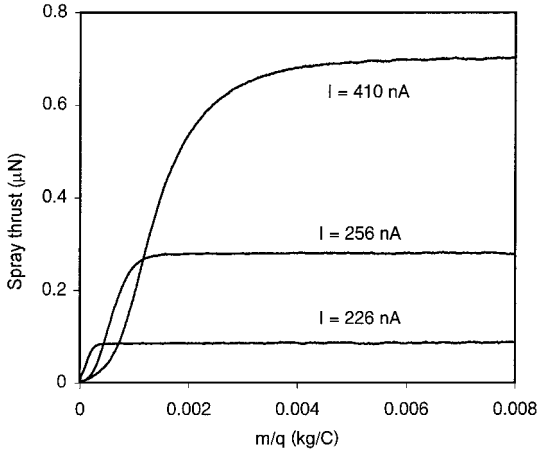


**Fig. 13 Thrust values rendered by TOF analysis for the sprays in Fig. 12.**

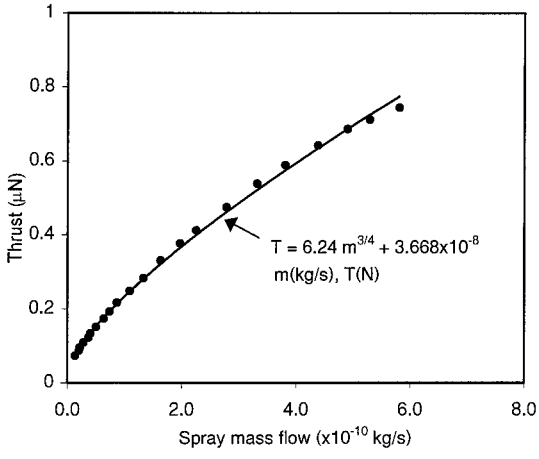


**Fig. 14 Thrust yielded by a single cone jet of F4 as a function of mass flow. The voltage of the needle is 1547 V, and the mean acceleration voltage is 1347 V.**

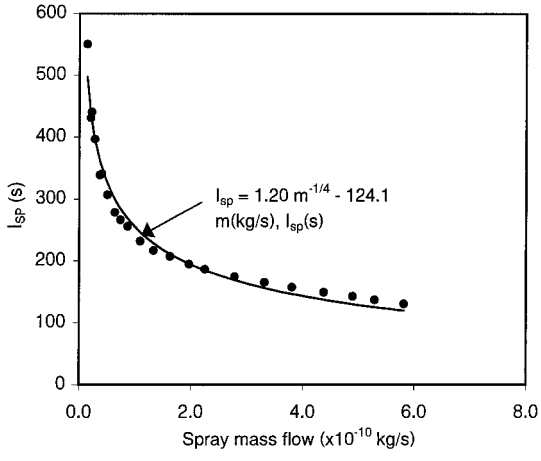


**Fig. 15 Specific impulse of F4 cone jets set at the same conditions as in Fig. 14.**

collect the thrusts and specific impulses of all of the F4 sprays studied, at an acceleration voltage of 1347 V. Although the lowest flow rate in these graphs is the minimum at which a stable cone jet could be set, flow rates larger than the largest shown are still possible. Curves fitting the experimental data are offered to allow the extrapolation of $T$ and $I_{sp}$ at different $V_A$ and $\dot{m}$. The forms of the scaling laws (7) and (8) are used to model the data. Figure 16 shows the ratio

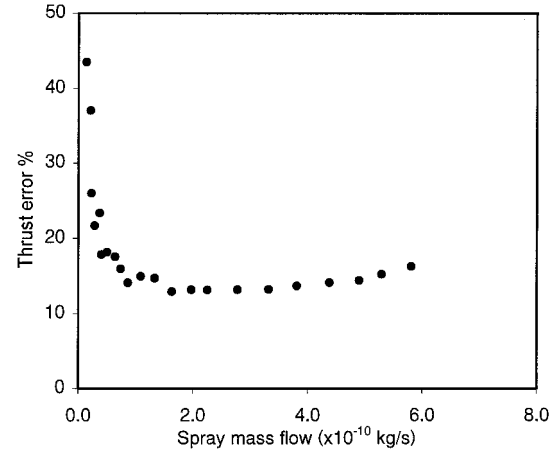


**Fig. 16 Error associated with using the average value of the specific charge to estimate spray thrust. The cone jets are those in Figs. 14 and 15.**

$$\text{Thrust error} = \{[\dot{m}\sqrt{2V_N(I/\dot{m})} - T]/T\} \times 100 \qquad (15)$$

i.e., the error involved in estimating the thrust using the average specific charge of the colloids and the needle voltage as the acceleration voltage. $\dot{m}$ and $T$ are the spray mass flow and the thrust yielded by the TOF measurement. At large flow rates the thrust computed by average values overestimates the measured value by 15% approximately, mainly because the voltage losses occurring in the electrospraying process are not included in the former. The overestimate is even larger for flow rates below $4.0 \times 10^{-11}$ kg/s. The error now is not only associated with voltage losses, but also with the important fraction of the current that is emitted in ionic form (see Fig. 9a): most of the mass is still emitted in the form of droplets, but their average specific charge is considerably lower than $I/\dot{m}$. Hence, the reduction in the thrust generated by the droplets cannot be compensated by the additional thrust produced by the ions because of the minute mass flow of the latter. This is readily seen for the ideal case of a spray formed by two types of particles, each one with a fixed specific charge. If we use $X$ and $Y$ to denote the mass flow and current fraction associated with one of the particle types and $I$ and $\dot{m}$ for the total current and mass flow of the spray, the combined thrust is simply

$$T = \dot{m}\left[\sqrt{2V_A XY(I/\dot{m})} + \sqrt{2V_A(1-X)(1-Y)(I/\dot{m})}\right] \qquad (16)$$

which reaches a maximum for $(X, Y)$ equal to either (1, 1) or (0, 0), i.e., for the case of a monodisperse spray. On the other hand, the thrust approaches 0 for $(X, Y)$ tending to (1, 0) or (0, 1), which is the trend observed in Fig. 16 for the lowest flow rates. The existence of several types of particles with different specific charges also reduces the efficiency of the spray. The efficiency of F4, defined in Eq. (12), is shown in Fig. 17. For $\dot{m}$ above $4.0 \times 10^{-11}$ kg/s, the efficiency has an approximately constant value of 76%. Again, this 25% drop is mostly caused by voltage losses in the cone jet: the average voltage loss is 200 V, 13% of the total needle voltage. The increasing relative importance of the ionic current below $\dot{m} = 4.0 \times 10^{-11}$ kg/s makes the efficiency lower because the extra thrust obtained from the solvated ions does not compensate the power required to accelerate them. Nevertheless, depending on the mission specifications propulsive efficiency might not be a relevant figure of merit in micropropulsion because of the low power requirements of these thrusters. Indeed, for propulsive needs requiring finely controllable and stable microthrusts (e.g., 20-$\mu$N nominal thrust with a noise lower than 0.1 $\mu$N) one can imagine that the power losses in the power processing unit will be comparable to the power spent in accelerating the electrospray. In this case the specific impulse, which measures the efficient use of propellant mass, and the thrust noise are parameters much more relevant than the propulsive efficiency. We have monitored the electric current emitted by a cone jet of F4 to compute

**Table 2 Colloid beam's characteristics of interest in electrostatic propulsion**

| Solution | $\dot{m}_{TOF}$, $\times 10^{-9}$ kg/s[a] | $\dot{m}_{FMT}$, $\times 10^{-9}$ kg/s[b] | $I$, nA | $V_N$, V | $T$, $\mu$N | $I_{sp}$, s | $\eta$,% | $(m/q)$, g/C |
|---|---|---|---|---|---|---|---|---|
| F1 | 1.14 | 1.20 | 260 | 1547 | 0.873 | 77.9 | 83.4 | 4.52 |
| F1 | 0.85 | 0.93 | 225 | 1547 | 0.693 | 83.0 | 81.0 | 5.05 |
| F1 | 0.50 | 0.55 | 164 | 1547 | 0.453 | 92.0 | 80.4 | 4.42 |
| F1 | 0.18 | 0.22 | 101 | 1547 | 0.215 | 124 | 80.5 | 2.30 |
| F2 | 0.65 | 0.71 | 367 | 1703 | 0.825 | 129 | 83.1 | 1.54 |
| F2 | 0.38 | 0.42 | 290 | 1703 | 0.559 | 149 | 82.8 | 1.26 |
| F2 | 0.19 | 0.23 | 209 | 1688 | 0.330 | 179 | 82.1 | 1.26 |
| F2 | 0.061 | 0.11 | 148 | 1672 | 0.152 | 255 | 75.7 | 0.72 |
| F3 | 0.65 | 0.69 | 445 | 1641 | 0.848 | 133 | 75.7 | 1.31 |
| F3 | 0.28 | 0.33 | 332 | 1641 | 0.489 | 179 | 78.9 | 0.79 |
| F3 | 0.064 | 0.11 | 202 | 1641 | 0.180 | 287 | 76.5 | 0.44 |
| F3 | 0.0069 | 0.026 | 272 | 1641 | 0.061 | 894 | 59.5 | 0.086 |
| F4 | 0.53 | 0.56 | 410 | 1547 | 0.711 | 137 | 75.2 | 0.11 |
| F4 | 0.13 | 0.17 | 256 | 1547 | 0.283 | 222 | 76.2 | 0.50 |
| F4 | 0.040 | 0.079 | 201 | 1547 | 0.134 | 341 | 71.4 | 0.21 |
| F4 | 0.021 | 0.045 | 226 | 1547 | 0.088 | 427 | 53.4 | 0.16 |
| Emi-Im | 0.51 | 0.53 | 307 | 1828 | 0.628 | 126 | 68.4 | 1.60 |
| Emi-Im | 0.21 | 0.20 | 216 | 1828 | 0.352 | 171 | 73.6 | 1.22 |
| TBP1 | 10.6 | 11.3 | 103 | 1547 | 1.585 | 15.2 | 79.5 | 155 |
| TBP1 | 1.52 | 1.58 | 43.4 | 1547 | 0.422 | 28.3 | 87.3 | 37.5 |
| TBP2 | 3.34 | 3.60 | 185 | 1469 | 1.21 | 36.9 | 80.6 | 15.9 |
| TBP2 | 1.17 | 1.14 | 116 | 1469 | 0.587 | 51.1 | 86.1 | 14.0 |
| TBP3 | 0.18 | 0.18 | 69 | 1453 | 0.176 | 99.7 | 86.7 | 3.42 |
| TBP3 | 0.078 | 0.070 | 45 | 1453 | 0.096 | 125 | 88.8 | 2.04 |
| TBP4 | 0.48 | 0.49 | 158 | 1516 | 0.437 | 92.8 | 83.3 | 3.27 |
| TBP4 | 0.079 | 0.079 | 64 | 516 | 0.114 | 147 | 84.8 | 1.69 |

[a]Mass flow rate obtained by integration of the TOF wave [Eq. (10)]. [b]Mass flow rate measured with bubble flow meter.

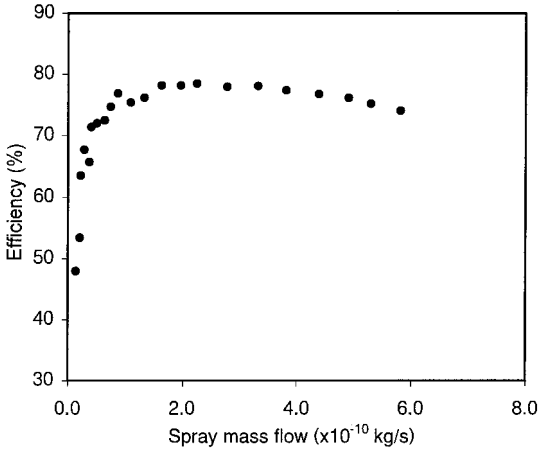


**Fig. 17 Efficiency of F4 cone jets. Thrust and mass flows are computed using the TOF curves of the sprays.**

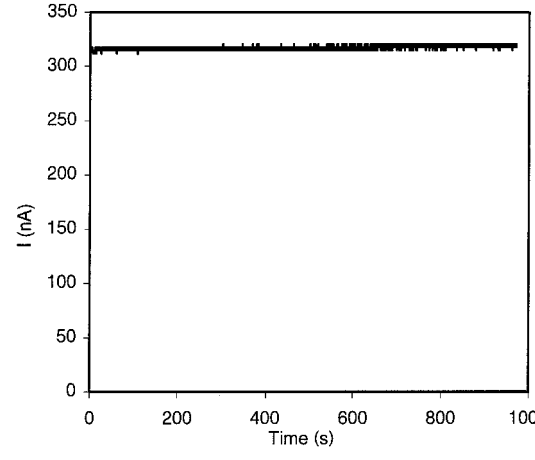


**Fig. 18 Time variation of the current emitted by a typical cone-jet of solution F4.**

the thrust noise related to time variations of the colloid beam. The evolution of $I$ during a time interval of 1000 s is shown in Fig. 18. Fifty samples per second were recorded. The mean values of $I$ and $\dot{m}$ are $\langle I\rangle = 317.38$ nA and $\langle \dot{m}\rangle = 2.37 \times 10^{-10}$ kg/s, and the standard deviation of the data in Fig. 18 is $\sigma_I = 1.790$ nA. The $T - \dot{m}$ fitting in Fig. 14 can be used to compute the mean value of the thrust, which is $\langle T\rangle = 0.413$ $\mu$N. With these data we can compute the standard deviation of $T$, which is simply given by

$$\sigma_T = \left.\frac{\mathrm{d}T}{\mathrm{d}I}\right|_{\langle I\rangle} \sigma_I \tag{17}$$

To obtain this expression, we have made use of the fact that $\sigma_I/\langle I\rangle$ and $\sigma_T/\langle T\rangle$ are much smaller than one. Finally we use the $I - \dot{m}$ and $T - \dot{m}$ fitting from Figs. 9a and 14 to compute the derivative in Eq. (17), and the estimate for $\sigma_T$ is $4.44 \times 10^{-3}$ $\mu$N. This thrust noise is certainly small and should not vary for the case of an array of individual cone jets, which will be needed to reach the thrust requirements of hypothetical missions.

### C. Characteristics of Several Propellants

Typical values of thrust, specific impulse, and efficiency for different electrosprays are given in Table 2. Other parameters of relevance such as the mass flow rate [measured by means of both TOF technique, Eq. (10), and bubble flow meter, the former is used to compute $I_{sp}$ and $\eta$), spray current, needle voltage, and specific charge of the main droplets are provided as well. TBP is a good propellant from the point of view of its low vapor pressure and relatively low viscosity coefficient. Unfortunately, its modest dielectric constant (8.9 at 25°C) prevents mixtures based on TBP and common salts to reach the high electrical conductivities desired for colloid thrusters. Thus, the specific charge of TBP droplets is too low to obtain interesting specific impulses at reasonable acceleration voltages. However, when TBP is mixed with important amounts of Emi-Im, the electrical conductivity of the resulting solution approaches the lower conductivity limit of interest (see Table 1). TBP cone-jets offer a good example of the high propulsive efficiency associated with colloid thrusters, which is a consequence of both the narrow specific charge distribution of the electrospray particles and the modest voltage losses as compared to typical acceleration voltages. It is worth

pointing out the similarity between the mass flow rates yielded by TOF and flow-meter measurement. Because both $\dot{m}_{\mathrm{TOF}}$ and $T$ are computed using the same scheme, i.e., the integrals in Eqs. (9) and (10), the validation of the former provides confirmation for the latter.

Data for the ionic liquid Emi-Im are also given in Table 2. These electrosprays have an ion emission regime similar to that shown in Fig. 7 for the case of F4 at high flow rate. However, the conductivity of Emi-Im at the temperature at which the experiments were done was too low to reach the dominating ion evaporation regime typical of low flow rates. Although these values of $I_{\mathrm{sp}}$ are still low for electrostatic thrusters (for example, the $I_{\mathrm{sp}}$ for $\dot{m} = 2.1 \times 10^{-10}$ kg/s at $V_A = 5000$ V is 292 s), we expect that mixtures of this or other ionic liquids with appropriate solvents, or higher working temperatures, will make ionic liquids attractive propellant candidates for this application. Again, the very similar values for the two independent measurements of $\dot{m}$ confirm both the suitability of the TOF technique and the virtual lack of liquid evaporative losses from the ionic liquid cone-jet.

The largest subset of data in Table 2 is associated with formamide solutions of different conductivities. Clearly the most interesting results are those of the solutions with higher $K$, which offer the specific impulses attractive in electrostatic propulsion. $I_{\mathrm{sp}}$ of some 500 s and above at $V_N \sim 1600$ V are achieved for the most conducting formamide solutions at the lowest flow rates. The wide range of thrust delivered by a single electrospray source within the window of flow rates allowing stable operation is noteworthy. The efficiencies are in most cases in the high seventies, dropping to about 50% when the evaporation of solvated ions begins to dominate the charge emission process. Unfortunately, the losses of formamide by evaporation from the cone-jet surface are important at the lowest flow rates (compare the data for $\dot{m}_{\mathrm{FMT}}$ and $\dot{m}_{\mathrm{TOF}}$ Table 2). In fact, we have measured a deficit between $\dot{m}_{\mathrm{FMT}}$ and $\dot{m}_{\mathrm{TOF}}$ of approximately $4 \times 10^{-11}$ kg/s regardless of the flow rate and solution conductivity. This is consistent with the scenario of formamide evaporating from a surface of constant area (the same electrospraying needle, i.d. $= 22$ $\mu$m, was used for every cone jet of formamide, and thus the area of every liquid meniscus was roughly the same). To solve this problem, the use of smaller needles or propellants of similar conductivities but with lower vapor pressure will be required (e.g., ionic liquids).

## V. Conclusions

We have studied electrosprays held in a vacuum by means of time of flight and stopping potential techniques. This combination provides a good understanding of the colloid beam properties and yields accurate measurements of the spray thrust and specific impulse. Cone-jets of highly conducting liquids operated at safe onset voltages offer the possibility of generating colloids with the specific charge required for electric propulsion. For example, a cone-jet of formamide with a conductivity of 1.5 S/m and operated at a flow rate and onset voltage of $4.0 \times 10^{-11}$ kg/s and 1547 V produces a beam of droplets with specific charge of 4760 C/kg. The thrust and specific impulse of that spray are 0.134 $\mu$N and 341 s. These values will raise up to 0.258 $\mu$N and 657 s if an acceleration voltage of 5000 V is applied to the spray by an acceleration electrode. Still higher specific impulses are reported in this article. The thrust noise related to variations of the colloid beam is of the order of $4 \times 10^{-3}$ $\mu$N.

The thrust and specific impulse delivered by a cone jet depend mainly on the electrical conductivity and flow rate of the electrosprayed solution. $T$ and $I_{\mathrm{sp}}$ vary with the mass flow rate as $\dot{m}^{3/4}$ and $\dot{m}^{-1/4}$, respectively. Thus, it is possible to obtain a wide range of the thrust delivered by a given cone-jet by controlling its flow rate. Unfortunately the specific impulse does not remain constant in the window of mass flow operation. Close to the minimum flow rate, $T$ and $I_{\mathrm{sp}}$ have a $K^{-1/2}$ and $K^{1/2}$ dependencies on electrical conductivity. Hence, from the point of view of specific impulse solutions with large electrical conductivities are most convenient.

For very conductive solutions electrosprayed close to the minimum flow rate, an important fraction of the total current is emitted in the form of solvated ions along with charged droplets. Although it would be interesting to work under conditions such that the emission were completely in the form of solvated ions, this regime has not been found yet for the case of electrosprays of organic liquids.

## Acknowledgments

We are indebted to M. Martinez-Sánchez (Massachusetts Institute of Technology) and J. Fernández de la Mora (Yale University) for numerous discussions on the subject. They both form part of this project for the study of colloid thrusters, and without their contributions the work presented in this article would have not been possible. In particular, one of the authors (M. G. C.) is most grateful for the help and guidance generously provided by J. Fernández de la Mora during recent years.

This research is supported by a NASA Phase II SBIR contract. We greatly acknowledge the support given by J. Sovey, NASA technical monitor of this contract.

## References

[1] Taylor, G. I., "Disintegration of Water Drops in an Electric Field," *Proceedings of the Royal Society of London* A, Vol. 280, No. 1382, 1964, pp. 383–397.

[2] Zeleny, J., "The Electrical Discharge from Liquid Points, and a Hydrostatic Method of Measuring the Electric Intensity at Their Surfaces," Physical Review, Vol. 3, No. 2, 1914, pp. 68–91.

[3] Zeleny, J., "On the Conditions of Instability of Electrified Drops, with Applications to the Electrical Discharge from Liquid Points," *Proceedings of the Cambridge Philosophical Society*, Vol. 18, 1915, pp. 71–83.

[4] Cloupeau, M., and Prunet-Foch, B., "Electrostatic Spraying of Liquids in Cone-Jet Mode," *Journal of Electrostatics*, Vol. 22, No. 2, 1989, pp. 135–159.

[5] Cloupeau, M., and Prunet-Foch, B., "Electrostatic Spraying of Liquids: Main Functioning Mode," *Journal of Electrostatics*, Vol. 25, No. 2, 1990, pp. 165–184.

[6] Krohn, V. E., "Liquid Metal Droplets for Heavy Particle Propulsion," *Progress in Astronautics and Rocketry*, Vol. 5, A. C. Press, New York and London, 1961, pp. 73–80.

[7] Krohn, V. E., "Glycerol Droplets for Electrostatic Propulsion," ARS Electric Propulsion Conf., Berkeley, CA, 1962.

[8] Huberman, M. N., and Rosen, S. G., "Advanced High-Thrust Colloid Sources," *Journal of Spacecraft*, Vol. 11, No. 7, 1974, pp. 475–480.

[9] Huberman, M. N., "Measurement of the Energy Dissipated in the Electrostatic Spraying Process," *Journal of Applied Physics*, Vol. 41, No. 2, 1970, pp. 578–584.

[10] Kidd, P. W., and Shelton, H., "Life Test (4350 hrs.) of an Advanced Colloid Thruster Module," AIAA Paper 73-1078, Nov. 1973.

[11] Martinez-Sánchez, M., Fernández de la Mora, J., Hruby, V., Gamero-Castaño, M., and Khayms, V., "Research on Colloid Thrusters," *Proceedings of the 26th International Electric Propulsion Conference*, IEPC Paper 99-014, Kitakyushu, Japan, Oct. 1999.

[12] Fernández de la Mora, J., and Loscertales, I. G., "The Current Emitted by Highly Conducting Taylor Cones," *Journal of Fluid Mechanics*, Vol. 260, Feb. 1994, pp. 155–184.

[13] Rosell-Llompart, J., and Fernández de la Mora, J., "Generation of Monodisperse Droplets 0.3 to 4 mm in Diameter from Electrified Cone-Jets of Highly Conducting and Viscous Liquids," *Journal of Aerosol Sciences*, Vol. 25, No. 6, 1994, pp. 1093–1119.

[14] Gañán-Calvo, A. M., Dávila, J., and Barrero, A., "Current and Droplet Size in the Electrospraying of Liquids. Scaling Laws," *Journal of Aerosol Sciences*, Vol. 28, No. 2, 1997, pp. 249–275.

[15] Chen, D. R., and Pui, D., "Experimental Investigation of Scaling Laws for Electrospraying: Dielectric Constant Effect," *Aerosol Science Technology*, Vol. 27, No. 3, 1997, pp. 367–380.

[16] Hines, R. L., "Electrostatic Atomization and Spray Painting," *Journal of Applied Physics*, Vol. 37, No. 7, 1966, pp. 2730–2736.

[17] Gañán-Calvo, A. M., "Cone-Jet Analytical Extension of Taylor's Electrostatic Solution and the Asymptotic Universal Scaling Laws in Electrospraying," *Physical Review Letters*, Vol. 79, No. 2, 1997, pp. 217–220.

[18] Cherney, L., "Structure of Taylor Cone-Jets. Limit of Low Flow Rates," *Journal of Fluid Mechanics*, Vol. 378, Jan. 1999, pp. 167–196.

[19] Hartman, R. P. A., Brunner, D. J., Camelot, D. M. A., Marijnissen, J. C. M., and Scarlett, B., "Electrohydrodynamic Atomization in the Cone-Jet Mode, Physical Modeling of the Liquid Cone and Jet," *Journal of Aerosol Sciences*, Vol. 30, No. 7, 1999, pp. 823–849.

[20] Hartman, R. P. A., Brunner, D. J., Camelot, D. M. A., Marijnissen, J. C. M., and Scarlett, B., "Jet Break-Up in Electrohydrodynamic Atomization in the Cone-Jet Mode," *Journal of Aerosol Sciences*, Vol. 31, No. 1, 2000, pp. 65–95.

[21] Gamero-Castaño, M., and Fernández de la Mora, J.,"Direct Measurement of Ion Evaporation Kinetics from Electrified Liquid Surfaces," *Journal of Chemical Physics,* Vol. 113, No. 2, 2000, pp. 815–832.

[22] Iribarne, J. V., and Thomson, B. A., "On the Evaporation of Small Ions from Charged Droplets," *Journal of Chemical Physics*, Vol. 64, No. 6, 1976, pp. 2287–2294.

[23] Hunter, R. E., and Wineland, S. H., "Charged Colloid Generation Research," Space Electronics Symposium, Los Angeles, 1965.

[24] Gamero-Castaño, M., "The Transfer of Ions and Charged Nanoparticles from Solution to the Gas Phase in Electrosprays," Ph.D. Dissertation, Dept. of Engineering and Applied Sciences, Yale Univ., New Haven, CT, Dec. 1998.

[25] McEwen, A. B., Ngo, H. L., LeCompte, K., and Goldman, J. L., "Electrochemical Properties of Imidazolium Salt Electrolytes for Electrochemical Capacitor Applications," *Journal of the Electrochemical Society*, Vol. 146, No. 5, 1999, pp. 1687–1695.

[26] Loscertales, I. G., and Fernández de la Mora, J., "Experiments on the Kinetics of Field Evaporation of Small Ions from Droplets," *Journal of Chemical Physics*, Vol. 103, No. 12, 1995, pp. 5041–5060.

[27] Riddick, J. A., and Bunger, W. B., *Organic Solvents. Physical Properties and Methods of Purification*, 3rd ed., Wiley, New York, 1970, pp. 323, 444.

[28] De Juan, L., and Fernández de la Mora, J., "Charge and Size Distribution of Electrospray Drops," *Journal of Colloidal and Interface Science*, Vol. 186, 1997, pp. 280–293.

[29] Lopez-Herrera, J. M., Gañán-Calvo, A. M., and Perez-Saborido, M., "One-Dimensional Simulation of the Breakup of Capillary Jets of Conducting Liquids. Application to E.H.D. Spraying," *Journal of Aerosol Sciences*, Vol. 30, No. 7, 1999, pp. 895–912.